2021 43rd Annual International Conference of the
IEEE Engineering in Medicine & Biology Society (EMBC)
Oct 31 - Nov 4, 2021. Virtual Conference

Transfer Entropy between Intracranial EEG Nodes Highlights Network Dynamics that Cause and Stop Epileptic Seizures

Simon Wing, Kristin M. Gunnarsdottir, Jorge Gonzalez-Martinez, Sridevi V. Sarma

Abstract— **Transfer entropy (TE) is used to examine the connectivity between nodes and the roles of nodes in epileptic neural networks during rest, moments before seizure, during seizure, and moments after seizure. There is a set of nodes that dominate information flow to epileptogenic zone (EZ) nodes, regions that trigger seizure, and non-EZ nodes during rest. The TE from the dominant to the EZ nodes decreases shortly before a seizure event and reaches a minimum during seizure. During the seizure, the dominant nodes cease or only weakly interact with the EZ nodes. This supports the hypothesis that seizure occurs when some nodes stop inhibiting the EZ nodes. The TE from the dominant to the EZ nodes peaks immediately after seizure, suggesting that seizure may stop when the brain exerts the highest level of information flow/activation/communication to the EZ nodes. The information flow from the dominant to EZ nodes is different from that to non-EZ nodes. This TE dynamics entering and exiting seizures may identify more accurately the EZ nodes, which may improve surgical planning.**

I. Introduction

Over 30% of epilepsy patients have incapacitating seizures which cannot be completely controlled with medication [1]. For patients with medically refractory epilepsy (MRE), the most common treatment option is instead a surgical resection of the epileptogenic zone (EZ), which is defined as the minimal area of brain tissue responsible for generating the recurrent seizure activity [2]. A successful surgical outcome can only be achieved by completely resecting or disconnecting the EZ and thus relies heavily on precise localization of this region. Before the surgery, a hypothesis of the EZ is formulated through a comprehensive evaluation comprising various modalities such as scalp-electroencephalography (scalp-EEG), MRI, PET and SPECT. When non-invasive methods are discordant regarding the location of the EZ, invasive evaluation using intracranial EEG (iEEG) may be needed [2].

Following invasive electrode placement, patients remain in the hospital for days to weeks waiting for a sufficient number of seizure events [3], [4]. Clinicians then visually inspect hundreds of invasive iEEG signals, studying the onset of seizure events, which are marked by the early presence of abnormal activity such as bursts of high frequency oscillations (100-300Hz). EEG channels where these onset features first appear are commonly identified as the EZ. Unfortunately, surgical success rates vary between 20-80% [5], [6], which stems from the EZ being inaccurately, or incorrectly identified and thus not entirely removed.

A growing body of research studies epilepsy as a network disease and network-based measures are increasingly used to characterize the architecture of connectivity patterns in epilepsy patients [7]–[16]. Recent studies suggest that rather than being a single source, the EZ is itself a highly coupled network responsible for the generation and propagation of the seizure activity [17]. Thus, understanding of the underlying dynamics and directionality of information flow within the epileptic network, not just during a seizure, but also before and after, may shed light on the mechanism of seizure, understanding of seizure's semiology, and facilitate a more accurate identification of the EZ.

In this study, we develop a tool that utilizes information theory to determine the information flow and causal relationships among the nodes in the epileptic network during rest, moments before, during, and moments after seizure. We compute the transfer entropy (TE) among the nodes in the network which allows us to establish a pattern of interactions among the clinically annotated EZ and non-EZ nodes in the network. A capability is developed to distinguish EZ from non-EZ nodes.

II. Methods

A. SEEG Data

The data analyzed in this study were stereotactic-EEG (SEEG) recordings from two patients. All patients had focal MRE and underwent robotic SEEG for extra-operative monitoring followed by SEEG-guided laser ablation. The data were recorded using the Nihon Kohden 1200A EEG diagnostic and monitoring system (Nihon Kohden America, Foothill Ranch, CA, USA) at a sampling frequency of 1 kHz. One patient (patient A) had a successful surgical outcome, defined as seizure free (Engel class I [18]) at 12+ months post-operation. The other patient (patient B) only had a partially successful surgical outcome initially (Engel class II), but the patient had a second surgery, which was successful (Engel class I).

B. Data Pre-processing

The data are bandpass filtered between 0.5 and 300 Hz with a fourth order Butterworth filter, and notch filtered at 60 Hz. A common average reference is applied to remove common noise from the signals. Finally, SEEG channels not recording from grey matter or otherwise deemed "bad" (e.g., broken or excessively noisy) by visual inspection are discarded from each patient's dataset.

C. Transfer Entropy (TE)

A common method to establish relationships between two variables in time series data is to use time shifted cross-correlation. However, cross-correlation can only establish

S. Wing, K.M. Gunnarsdottir, and S. V. Sarma are with Johns Hopkins University, Baltimore, MD, USA. Contact: Simon.Wing@jhuapl.edu

J. Gonzalez-Martinez is with University of Pittsburgh Medical Center, Pittsburgh, PA, USA

978-1-7281-1178-0/21/$31.00 ©2021 IEEE

linear relationships and cannot establish causalities. A better alternative is to use TE [19]. TE($x \rightarrow y$) gives a measure of information transfer from variable x to y, given all the past values of y are known. TE has often been used to establish causality [20], [21] and can work for linear and nonlinear systems [20], [22]. TE has offered insights into the functional connectivity of systems in a variety of fields, including neurology and space science [23]–[28].

is an EZ channel and x is a non EZ channel. The mean noise, σ, and S are computed for each TE. Figure 1 a–g show an example of the result of applying TE from every channel to the EZ channel L'3, which is referred to herein as TE map for L'3.

Figure 1a shows that during rest, TEs are generally low to moderate. The channels with the highest TEs are channels 48–50 (G'12–14) at most τ. These 3 channels consistently dominate the information transfer to EZ as well as non-EZ

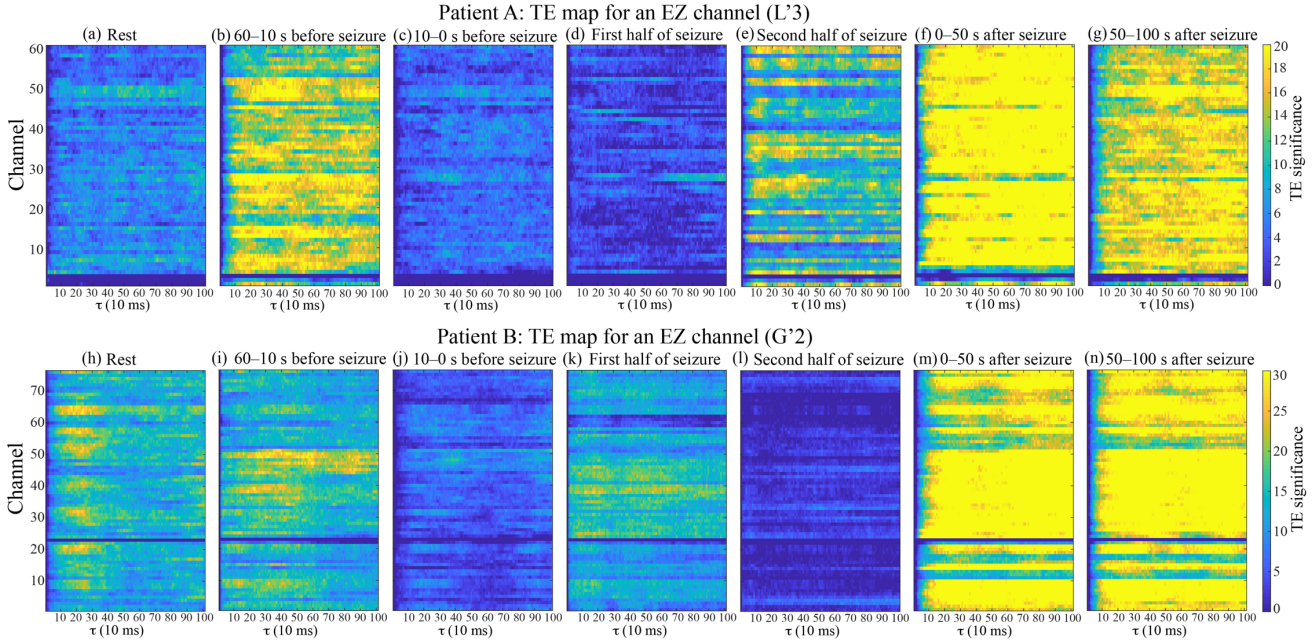

Figure 1. TE maps for an EZ channel for patients A (a–g) and B (h–n). In each map, the x axis is τ, y axis is the channel number, and the color is TE S.

For the present study, we identify seven time intervals of interest: (a) rest, (b) 60–10 s before onset of seizure, (c) 10–0 s before onset, (d) first half of seizure, (e) second half of seizure, (f) 0–50 s after the end of seizure, and (g) 50–100 s after seizure. Rest is the time when there is no seizure, typically hours before a seizure event. We apply TE($x \rightarrow y$)(τ) where x and y are the time series electrode signals from two different channels in the SEEG data and τ is the response lag time. Noise in the system is computed from surrogate data, sur(x), which is obtained by randomly permutating the order of x. The mean noise and σ are determined from an ensemble of 100 permutations of TE(sur(x) $\rightarrow$ y)(τ), from which we calculate significance S = (TE – mean noise)/σ. In the network analogy, each SEEG channel is a node in the neural network. Significant TE($x \rightarrow y$) suggests that node x activates node y (x causes y to change), which can include positive (excitation) or negative activation (inhibition). The strength of the causal connection can be measured by S. In order save computational time, we average the data using 10 ms window moving average. The results do not change significantly from those computed with 1 ms time resolution.

III. Results

A. Patient A – Successful outcome after one surgery

The clinicians inserted electrodes with 60 contacts in the brain of patient A corresponding to 60 channels, 3 of which have been identified as EZ channels (labeled as L'2, L'3, and L'4). We apply TE(x $\rightarrow$ y)(τ) for the 7 time intervals, where y channels. At 60–10 s before seizure, TEs for many channels, including G'12–14, increase (Figure 1b), but at 10–0 s before seizure, the TEs dramatically decrease (Figure 1c). However, G'12–14 still dominate information flow to EZ channels albeit their TEs are lower.

In the first half of seizure, TEs for most channels decrease even further and reach a minimum (Figure 1d). Interestingly, this time, the TEs for G'12–14 are lower than those for most channels. In the second half of seizure, while TEs for many channels have increased, TEs for G'12–14 still remain among the lowest (Figure 1e).

In the immediate aftermath of seizure, at 0–50 s after the seizure, TEs for most channels increase dramatically (Figure 1f). Their values are off the chart. At 50–100 s after seizure, TEs start to decrease, perhaps reverting back to the resting state (Figure 1g). G'12–14 return to dominate the information flow to the EZ channels.

We have computed the TE maps for the other two EZ channels (L'2 and L'4), and they follow a similar pattern as that of L'3. This is summarized in Figure 2a, which plots the median TE from the dominant channels to all 3 EZ channels (red curve). It shows that TE is moderate during rest, increases at 60–10 s before onset, decreases significantly at 10–0 s before onset, reaches a minimum near 0 in the first half of seizure, increases slightly in the second half of seizure, and increases dramatically immediately after seizure (0–50 s after seizure), and decreases at 50–100 s after seizure.

To show the dominance of G'12–14, Figure 2a plots the median TE of other channels (non G'12–14) to EZ channels (blue curve). The figure shows that the blue curve is generally lower than the red curve, except during the seizure, which may have implications to the seizure dynamics as described next.

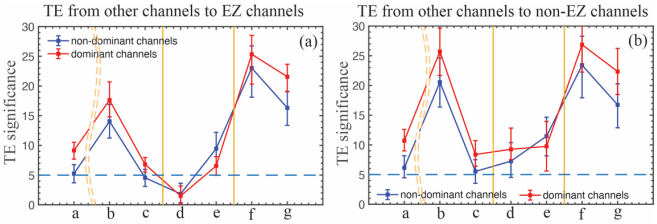

Figure 2. (a) Median TE from the dominant channels to the EZ channels (red curve) and median TE from non-dominant channels to the EZ channels (blue curve). The error bars are the first and third quartiles. (b) the same as (a) except for randomly selected non-EZ channels. Seizure occurs between the two vertical orange lines. The x axis is time: a = rest, b = 60–10 s before seizure, c = 10–0 s before seizure, d = first half of seizure, e = second half of seizure, f = 0–50 s after seizure, g = 50–100 s after seizure.

Figures 1 and 2a suggest that in terms of connectivity between nodes, G'12–14 dominate the information flow to the EZ nodes during rest and moments before seizure. Seizure occurs when these nodes transfer little information to EZ nodes and cease to dominate. Seizure stops when G'12–14 and other nodes more strongly than ever transfer information to the EZ nodes. As the network goes back to the resting state, G'12–14 again assert their dominance. This observed pattern supports the hypothesis that during rest, the EZ nodes are being inhibited by functional neighbors, and that a seizure occurs because these neighboring nodes stop inhibiting the EZ nodes [29], [30].

The pattern described above is subtly different for non-EZ nodes. To illustrate, we randomly select 4 nodes to represent non-EZ nodes and compute TEs from G'12–14 and other nodes to these non-EZ nodes. The medians are plotted in Figure 2b. The TE for the dominant nodes is still larger than that for non-dominant nodes. Comparisons of Figures 2a and 2b show 2 key differences: (1) the minimum TE is reached during seizure for EZ nodes whereas the minimum is reached at 10–0 s before seizure for non-EZ nodes; and (2) TE after seizure is significantly higher than that before seizure for EZ nodes, but this is not the case for non-EZ nodes. The latter may signify that the brain makes a concerted effort, more than at any other times, to inhibit the EZ nodes to stop the seizure. On the other hand, for non-EZ nodes, the TE is fairly similar before and after seizure.

B. Patient B – Successful outcome after two surgeries

We perform the same calculation for Patient B data. Patient B has 76 channels and 12 EZ nodes were identified by clinicians.

Figure 1 h–n shows an example of the TE maps for an EZ channel (G'2). The pattern is similar to that seen in Figure 1 a–g with a few exceptions as discussed next.

Figure 3a summarizes the dynamical pattern as done in Figure 2a. In comparison with patient A, the TE at rest for patient B starts at a high level. It is unknown when the resting state period was taken relative to seizure for patients A and B. Perhaps, the resting state period for patient B was closer to the seizure event, which may explain the high level of TE. In any case, the TE for 60–10 s before onset is only slightly higher than that for rest. As for patient A, TE drops significantly just before onset. In the first half of seizure, TE increases. Its significance is not clear. It may suggest that the brain attempts to inhibit the EZ nodes, but fails. TE reaches the minimum only in the second half seizure. Immediately after seizure, TE reaches the maximum, as with patient A.

As done for patient A, we apply TE to 6 randomly selected non-EZ nodes. Figure 3b plots the median TE for non-EZ channels, which can be compared to Figure 2b. The characteristics of the two plots are similar, except that in Figure 3b, TE peaks in the first half of seizure and the minimum TE is lower. A key similarity is that the TE immediately after seizure is the about the same as that before seizure.

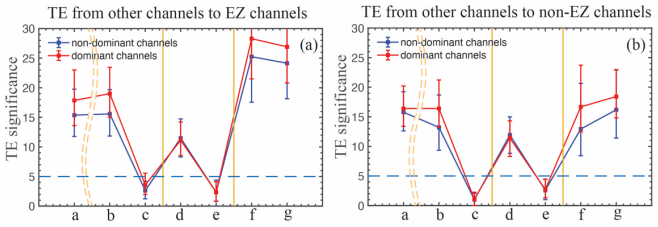

Figure 3. The same as Figure 2, except for patient B. The x axis is time and described in Figure 2 caption.

As mentioned in Section II.A, although the patient improved after the first surgical procedure, the patient needed a second procedure to achieve complete success. 16 additional nodes were identified as EZ for the second procedure.

We examine the second set of EZ nodes and find that indeed, some of the nodes have the same EZ signature shown in Figures 2a and 3a. An example is shown in Figure 4a. However, some of the nodes do not, an example of which is shown in Figure 4b.

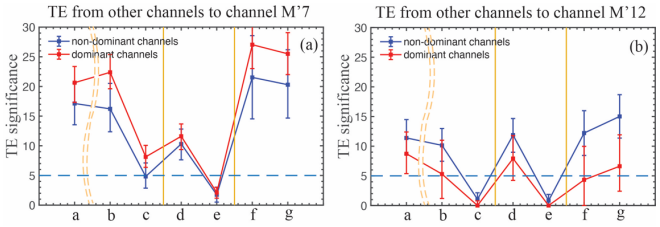

Figure 4. (a) an example of an EZ node (M'7) that has the EZ signature in. (b) an example of an EZ node (M'12) that does not have the EZ signature. See Figure 2 caption for the the plot description, including the x axis labels.

IV. Discussion and Conclusion

We examine the connectivity between nodes and the roles of nodes in the epileptic neural networks during rest, moments before seizure, during seizure, and moments after seizure. There is a set of nodes that dominate the information flow to EZ and most other nodes during rest. This may suggest that some regions of the brain (dominant nodes) inhibit the EZ during rest. The TEs from the dominant nodes to EZ nodes look different from those to non-EZ nodes. The TE dynamics before, during and after seizures are summarized in Table 1. The TE dynamics of the EZ nodes appear to have a consistent signature and may facilitate a more accurate identification of

the EZ nodes.

TABLE 1. TE FROM DOMINANT NODES TO EZ AND NON-EZ NODES

Time	EZ nodes	non-EZ nodes
–60 to –10 s	increase, dominate	may increase
–10 to 0 s	decrease, dominate	reach min
during seizure	reach min, cease to dominate	slightly increase
0 to 50 s	reach max, resume dominating	increase to ~TE for –60 s
50 to 100 s	decrease, dominate	may decrease

Our analysis suggests that (1) **seizure occurs** when the dominant nodes cease to dominate the information flow or weakly transfer information to the EZ nodes, supporting the hypothesis that seizure occurs when some nodes stop inhibiting the EZ nodes [29], [30]; (2) **seizure stops** when the dominant and other channels strongly increase the activation of or information flow/ communication to the EZ nodes, much more strongly than at any other times. It may suggest that this level of effort is needed to stop the seizure. The effort seen at 60–10 s before seizure is high, but perhaps not high enough to suppress seizure. It may signify that the brain recognizes that seizure is looming and attempts to stop it, but the effort apparently is not strong enough. For non-EZ nodes, TE increases after seizure, but it increases to about the same level as before seizure. Thus, if the seizure could be stopped by this level of TE to non-EZ nodes, it would have stopped seizure at 60–10 s before seizure.

The nodes that are identified as EZ by their TE signature (as described in Table 1) match well with the EZ nodes identified by clinicians when the surgical procedure is a success (as in patient A). However, for patient B, we find that there are a few TE EZ nodes that are not in the clinically annotated list of EZ nodes for the first procedure, which may explain why the first surgery was only partially successful (Engel class II). These TE EZ nodes are included in the second procedure and the patient achieved Engel class I afterward. There are, however, a few clinically annotated EZ nodes in the second procedure that do not match the TE EZ signature. This suggests that TE may be able to refine the boundary of the EZ and improve planning for surgical procedures.

The present study has only analyzed two patients. We plan to analyze more patients in our follow up study. It would be interesting also to examine TE from EZ to other nodes.

ACKNOWLEDGMENT

S. Wing acknowledges the support of the Sabbatical Fellowship at the Johns Hopkins University Applied Physics Laboratory (JHU/APL).

REFERENCES

[1] P. Kwan and M. J. Brodie, "Definition of refractory epilepsy: defining the indefinable?," *Lancet Neurol.*, vol. 9, no. 1, pp. 27–29, Jan. 2010, doi: 10.1016/S1474-4422(09)70304-7.

[2] F. Rosenow and H. Lüders, "Presurgical evaluation of epilepsy," *Brain*, vol. 124, no. 9, pp. 1683–1700, Sep. 2001, doi: 10.1093/brain/124.9.1683.

[3] P. Widdess-Walsh, L. Jeha, D. Nair, P. Kotagal, W. Bingaman, and I. Najm, "Subdural electrode analysis in focal cortical dysplasia: predictors of surgical outcome," *Neurology*, vol. 69, no. 7, pp. 660–667, Aug. 2007, doi: 10.1212/01.wnl.0000267427.91987.21.

[4] I. M. Najm, W. E. Bingaman, and H. O. Lüders, "The use of subdural grids in the management of focal malformations due to abnormal cortical development," *Neurosurg. Clin. N. Am.*, vol. 13, no. 1, pp. 87–92, viii–ix, Jan. 2002, doi: 10.1016/s1042-3680(02)80009-2.

[5] L. E. Jeha, I. Najm, W. Bingaman, D. Dinner, P. Widdess-Walsh, and H. Lüders, "Surgical outcome and prognostic factors of frontal lobe epilepsy surgery," *Brain*, vol. 130, no. 2, pp. 574–584, Feb. 2007, doi: 10.1093/brain/awl364.

[6] W. L. Ramey, N. L. Martirosyan, C. M. Lieu, H. A. Hasham, G. M. Lemole, and M. E. Weinand, "Current management and surgical outcomes of medically intractable epilepsy," *Clin. Neurol. Neurosurg.*, vol. 115, no. 12, pp. 2411–2418, Dec. 2013, doi: 10.1016/j.clineuro.2013.09.035.

[7] W. Stacey *et al.*, "Emerging roles of network analysis for epilepsy," *Epilepsy Res.*, vol. 159, p. 106255, Jan. 2020, doi: 10.1016/j.eplepsyres.2019.106255.

[8] B. C. Bernhardt, L. Bonilha, and D. W. Gross, "Network analysis for a network disorder: The emerging role of graph theory in the study of epilepsy," *Epilepsy Behav.*, vol. 50, pp. 162–170, Sep. 2015, doi: 10.1016/j.yebeh.2015.06.005.

[9] A. Li *et al.*, "Using network analysis to localize the epileptogenic zone from invasive EEG recordings in intractable focal epilepsy," *Netw. Neurosci.*, vol. 2, no. 2, pp. 218–240, Jun. 2018, doi: 10.1162/netn_a_00043.

[10] D. S. Bassett and O. Sporns, "Network neuroscience," *Nat. Neurosci.*, vol. 20, no. 3, Art. no. 3, Mar. 2017, doi: 10.1038/nn.4502.

[11] A. N. Khambhati, K. A. Davis, T. H. Lucas, B. Litt, and D. S. Bassett, "Virtual Cortical Resection Reveals Push-Pull Network Control Preceding Seizure Evolution," *Neuron*, vol. 91, no. 5, pp. 1170–1182, Sep. 2016, doi: 10.1016/j.neuron.2016.07.039.

[12] A. Korzeniewska *et al.*, "Ictal propagation of high frequency activity is recapitulated in interictal recordings: Effective connectivity of epileptogenic networks recorded with intracranial EEG," *NeuroImage*, vol. 101, pp. 96–113, Nov. 2014, doi: 10.1016/j.neuroimage.2014.06.078.

[13] Burns SP, Santaniello S, Yaffe RB, Jouny C, Crone N, Bergey G, Anderson WS, Sarma SV. (2014) Network Dynamics of the Brain and Influence of the Epileptic Seizure Onset Zone. *Proc Natl Acad Sci* U S A. 2014 Dec 9;111(49):E5321-30. PMID: 25404339

[14] William Stacey, Mark Kramer, Kristin Gunnarsdottir, Jorge Gonzalez-Martinez, Kareem Zaghloul, Sara Inati, Sridevi Sarma, Jennifer Stiso, Ankit N. Khambhati, and Danielle S. Bassett, Rachel J. Smith, Virginia B. Liu, Beth A. Lopour, Richard Staba. Emerging roles of network analysis for epilepsy. Epilepsy Res. 2020 Jan;159:106255

[15] Li A, Chennuri B, Subramanian S, Yaffe R, Gliske S, Stacey W, Norton R, Jordan A, Zaghloul K, …, Sarma SV. Using Network Analysis to Localize the Epileptogenic Zone from Invasive EEG Recordings in Intractable Focal Epilepsy. *Netw Neurosci. 2018; 2(2): 218–240*

[16] Yaffe RB, Borger P, Megevand P, Groppe DM, Kramer MA, Chu CJ, Santaniello S, Meisel C, Mehta AD, Sarma SV (2014) Physiology of Functional and Effective Networks in Epilepsy. *Clin Neurophysiol.* 2015 Feb;126(2):227-36 PMID: 25283711

[17] E. van Diessen, S. J. H. Diederen, K. P. J. Braun, F. E. Jansen, and C. J. Stam, "Functional and structural brain networks in epilepsy: What have we learned?," *Epilepsia*, vol. 54, no. 11, pp. 1855–1865, 2013, doi: https://doi.org/10.1111/epi.12350.

[18] J. Jr. Engel, "Outcome with respect to epileptic seizures.," *Surg. Treat. Epilepsies*, pp. 609–621, 1993.

[19] Schreiber, T., Measuring Information Transfer, Physical Review Letters, 85, 461–464, 2000, doi: 10.1103/PhysRevLett.85.461.

[20] Granger, C. W. J. 1969 Investigating causal relations by econometric models and cross-spectral methods. Econometrica 37, 424-438.

[21] Granger, C. W. J. 1980 Testing for causality: A personal viewpoint. Journal of Economic Dynamics and Control 2, 329-352.

[22] Barnett, Lionel, Adam B. Barrett, and Anil K. Seth, Granger Causality and Transfer Entropy Are Equivalent for Gaussian Variables, Physical Review Letters. 103 (23): 238701. 2009, arXiv:0910.4514

[23] Ding, M., Y. Chen, and S. Bressler, Granger Causality: Basic Theory and Application to Neuroscience, in Handbook of Time Series Analysis, edited by S. Schelter, M. Winterhalder, and J. Timmer (Wiley, Wienheim, 2006), pp. 438–460.

[24] Seth, A. K., and G. Edelman, Distinguishing Causal Interactions in Neural Populations, Neural Comput. 19, 910 (2007).

[25] Cadotte, A. J., T. B. DeMarse, P. He, and M. Ding, Causal Measures of Structure and Plasticity in Simulated and Living Neural Networks, PLoS ONE 3, e3355 (2008)

[26] Wing, S.,J. R. Johnson, E. Camporeale, and G. D. Reeves, Information theoretical approach to discovering solar wind drivers of the outer radiation belt, J. Geophys. Res. Space Physics, 121, 9378–9399, 2016, doi:10.1002/2016JA022711

[27] Wing, S., J. Johnson, and A. Vourlidas (2018), Information theoretic approach to discovering causalities in the solar cycle, *Ap J*, **854,** 85, https://doi.org/10.3847/1538-4357/aaa8e7

[28] Wing, S., P. C. Brandt, D. G. Mitchell, J. R. Johnson, W. S. Kurth and J. D. Menietti (2020), Periodic Narrowband Radio Wave Emissions and Inward Plasma Transport at Saturn's Magnetosphere, Ap J, 159, 249, 10.3847/1538-3881/ab818d, https://doi.org/10.3847/1538-3881/ab818d.

[29] Chakravarthy N, Tsakalis K, Sabesan S, Iasemidis L. Homeostasis of brain dynamics in epilepsy: a feedback control systems perspective of seizures. Ann Biomed Eng. 2009;37(3):565–85. 46.

[30] Narasimhan S, Kundassery KB, Gupta K, Johnson GW, Wills KE, Goodale SE, Haas K, Rolston JD, Naftel RP, Morgan VL, Dawant BM, González HFJ, Englot DJ. Seizure-onset regions demonstrate high inward directed connectivity during resting-state: An SEEG study in focal epilepsy. Epilepsia. 2020 Sep 18. doi: 10.1111/epi.16686. Epub ahead of print. PMID: 32944945.